# Polarization effects in the ionization cross section for collisions of excited Ne**{(2p)5(3p); J = 3}) with Ar : a sensitive probe for "locking" phenomena

# Polarization Effects in the Ionization Cross Section for Collisions of $Ne^{**}\{(2p)^5(3p);J=3\}$ with Ar: A Sensitive Probe for "Locking" Phenomena

J. P. J. Driessen, F. J. M. van de Weijer, M. J. Zonneveld, L. M. T. Somers, M. F. M. Janssens, H. C. W. Beijerinck, and B. J. Verhaar

*Physics Department, Eindhoven University of Technology, P.O. Box 513, 5600 MB Eindhoven, The Netherlands*

(Received 7 March 1989)

At a collision energy $E=0.1$ eV we see a large polarization effect $Q_{ion}^{|M_J|=0,1}/Q_{ion}^{|M_J|=3}=2.5$, decreasing to 1.4 for $E\geq 1$ eV. A two-state basis is used for the autoionization width of the $\pi$ and $\sigma$ orientations of the $(2p)^{-1}$ core hole, resulting in a preference for the $\Omega=0,1$ molecular states as seen at 0.1 eV. The energy dependence is due to the decrease of "locking" of **J** to the internuclear axis with increasing angular velocity $\dot{\phi}$, leading to the semiclassical criterion $\omega_{prec}=4\dot{\phi}$ for the transition from a space-fixed to a body-fixed description of **J**.

PACS numbers: 34.50.Fa, 31.50.+w, 31.70.−f, 34.50.Rk

Polarization effects in inelastic collisions of electronically excited, open shell atoms are an important means to obtain detailed insight into the mechanisms governing the collision process.[1-6] In a collision experiment, the excited atom can be prepared in an initial state $|J,M_J\rangle_{\mathbf{g}}$ in a space-fixed frame, with the relative velocity **g** as a quantization axis. The inelastic process, however, is described in a body-fixed frame with quantum numbers $|J,\Omega\rangle_{z'}$ for the total electronic angular momentum $J$ and its orientation $\Omega$ with respect to the internuclear axis $z'$. The polarized-atom cross section $Q^{|M_J|}$ depends on two features. First, we need to know the spatial evolution of the asymptotic initial state $|J,M_J\rangle$ to the local molecular states $|J,\Omega\rangle$ along the particle trajectory, known as rotational coupling. Second, the inelastic processes have an $\Omega$-dependent probability, which in general is the main objective of our research.

In a semiclassical analysis both features must be incorporated. Accurate semiclassical models for the $\Omega$-dependent inelastic processes are widely available, e.g., the extended Landau-Zener models of Nikitin[7] and the optical potentials of Connor and Thylwe.[8] For rotational coupling, the situation is quite different. The concept of "locking," i.e., the coupling of **J** to the internuclear axis, has been used quite often.[9,10] A suitable recipe, however, is not readily available. Because of its large influence on the observed polarization effects, it is essential to investigate locking in detail.

To unravel these problems we have studied the energy dependence of the polarization effects in the total ionization cross section in a wide energy range $0.1\leq E$ (eV) $\leq 5$ for the $Ne^{**}\{(2p)^5(3p);J=3\}$-Ar system. Because, in general, the locking phenomena and the $\Omega$-dependent dynamics have a different dependence on collision energy $E$, this is the only approach that allows a separation of these two effects.

The experimental setup, described previously by Verheijen and Beijerinck[11] and van den Berg, Schonenberg, and Beijerinck,[12] consists of a crossed-beam apparatus. The primary beam flux and ion yield are measured with time-of-flight analysis. The two-level system $Ne^*\{(3s);J=2\}\leftrightarrow Ne^{**}\{(3p);J=3\}$ is excited by a single-mode cw dye laser at $\lambda=640$ nm with the wave vector **k** perpendicular to the collision plane. Both a linear polarization with different orientations of the electric field **E** in the collision plane and a circular polarization are used. The modulation of the ion yield (laser on and off, respectively) is a direct measure for the difference cross section $\Delta Q_{ion}^{\beta}={}^3Q_{ion}^{\beta}-{}^2Q_{ion}^{\beta}$, with $\beta$ the angle between **g** and **E** (**k** for circular polarization). The superscripts $J=3$ and 2 correspond to the upper and lower state, respectively. The effective cross section ${}^JQ_{ion}^{\beta}$ is a sum over the polarized-atom cross sections ${}^JQ_{ion}^{|M_J|}$ for asymptotic pure magnetic substates, with the weight factors determined by the process of optical pumping. Combining cross sections ${}^JQ_{ion}^{\beta}$ for several laser polarizations enables us to determine the ${}^JQ_{ion}^{|M_J|}$ values. The population ratio $Ne^*(3s):Ne^{**}(3p)=0.52:0.48$ has been calibrated by measuring the saturation curve of the total ion yield for $Ne^{**}$-$H_2$ collisions.

In Fig. 1 we show the energy dependence of the $M_J$-averaged ionization cross section ${}^JQ_{ion}$ for both states. At thermal energies we observe a larger cross section for the $Ne^{**}(3p)$ state, which correlates with the smaller distance of closest approach in comparison to the $Ne^*(3s)$ state. At energies in the eV range the role of the $3s$ or $3p$ valence electron is less important and the cross sections are nearly equal, implying the same shape of the repulsive branch of the potential in this range.

Varying the laser polarization has a rather small effect on the total ion yield, due to the isotopic (90% $^{20}Ne$, 10% $^{22}Ne$) and fine-structure-state composition ${}^3P_2:{}^3P_0=5:1$ of the metastable-atom beam. At thermal energies we find a 10% modulation of the total ion yield, when varying the angle $\beta$ between **E** and **g** from $\beta=0$ to $\pi/2$; at $E\simeq 1$ eV this modulation is only 1%. Deconvolution of these data result in an effective polarization effect ${}^3Q_{ion}^{\beta=0}/{}^3Q_{ion}^{\beta=\pi/2}=1.37\pm 0.02$ and $1.04\pm 0.03$ in the

 

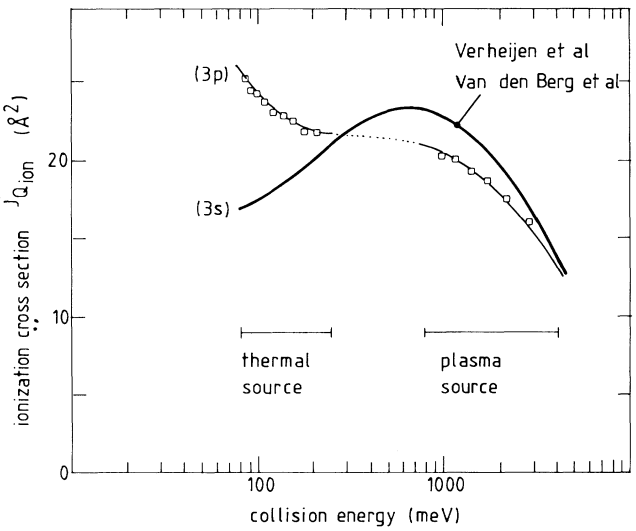


FIG. 1. Experimental results for the average ionization cross section $^{J}Q_{\text{ion}}$ for the metastable Ne*{(3$s$);$J=2$} and the short-lived Ne**{(3$p$);$J=3$} states both for Ar as a target.

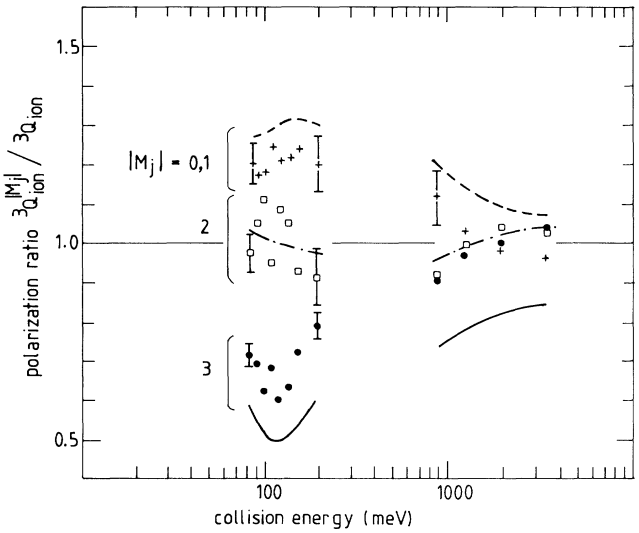


FIG. 2. Experimental results for the polarization effect in the ionization cross section for the Ne**{(3$p$);$J=3$)}-Ar system, deconvoluted while fully neglecting (data points) or using (line) the preliminary data of Ref. 13 for the lower-state polarization effect.

thermal and the eV energy range, respectively. The thermal data are in good agreement with the value $1.33 \pm 0.07$ of Bussert *et al.*[5]

The final results for the polarization ratio $^{3}Q_{\text{ion}}^{|M_J|}/{}^{3}Q_{\text{ion}}$ depend on the polarization effect for the lower-state cross section $^{2}Q_{\text{ion}}^{|M_J|}$ and are given in Fig. 2. First we have performed a $^{3}Q_{\text{ion}}^{|M_J|}$ analysis while neglecting the lower-state polarization effect (data points). In a second analysis we used preliminary results of Driessen, Janssens, and Beijerinck[13] indicating an energy-independent value $^{2}Q_{\text{ion}}^{0,1}/{}^{2}Q_{\text{ion}}^{2} \simeq 4/3$, which confirms similar data reported by Bregel[14] (curves). We see a large upper-state polarization effect with a local maximum at thermal energies. In the superthermal energy range both states have equal polarization effects.

To understand the different energy dependence of the polarization effects for both states we investigate the spatial dynamics of the total angular momentum **J**. For Ne*(3$s$) the $\Omega$ splitting of the adiabatic potentials is restricted to the repulsive branch. For Ne**(3$p$), however, the $\Omega$ splitting of the intermolecular potentials is much larger and is perceptible in the well area and even beyond (Fig. 3). In classical terms the $\Omega$-dependent potentials translate into a torque on **J** resulting in a precession with respect to the internuclear axis with frequency

$$\omega_{\text{prec}} = \Delta V^{\Omega,\Omega'}/\hbar \,. \tag{1}$$

Counteracting this precession, which would result in a well-defined quantum number $\Omega$ in the body-fixed system, is the rotation of the internuclear axis with an angular velocity $\dot{\phi}$,

$$\dot{\phi} = (N + \tfrac{1}{2})\hbar/\mu R^2 \,. \tag{2}$$

When $\omega_{\text{prec}} \ll \dot{\phi}$, the coupling to the internuclear axis is weak and a space-fixed description of **J** is favored. On the other hand, when $\omega_{\text{prec}} \gg \dot{\phi}$, a body-fixed description of **J** is correct. Our task is to determine a locking factor $f_L$, defined as

$$\omega_{\text{prec}} = f_L \dot{\phi} \,, \tag{3}$$

and a corresponding distance $R_L$ that can serve as an effective boundary between the two limiting cases. This is equal to a transition from Hund's case $e$ to case $c$, rather uncommon in molecular spectroscopy. In the ap-

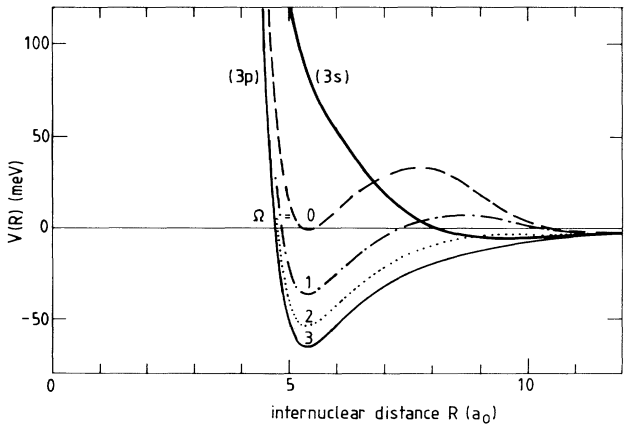


FIG. 3. Model potentials for the Ne**{(3$p$);$J=3$} state, calculated with the method of Masnou-Seeuws (Ref. 16) in combination with the 3$p$ input potentials of Bussert *et al.* (Ref. 5), in comparison with the best available Ne*(3$s$) potential of Gregor and Siska (Ref. 15).

proach of Nikitin the accumulated phase difference between the $\Omega$ and $\Omega'$ states is used as the criterion for locking. For a rather flat difference potential $\Delta V^{\Omega\Omega'}$ this is only a measure for depolarization, but does not ensure that the dynamical process of locking is effective. For example, this is the case for a rather flat difference potential $\Delta V^{\Omega\Omega'}$. Because $\Delta V^{\Omega,\Omega'}$ usually decreases exponentially, in comparison to the inverse square falloff of $\dot{\phi}$, both criteria will result in approximately the same value of the $R_L$.

To determine the locking factor $f_L$ and to test different assumptions for the $\Omega$ dependence of the process of ionization, we have performed a semiclassical model calculation for the Ne**-Ar system. The trajectory is calculated on an average adiabatic potential, using the $\Omega$-state populations as a weight factor. When $\omega_{\text{prec}} < f_L\dot{\phi}$ the evolution of the initial $|J,M_J\rangle_g$ state is calculated along the trajectory at fixed steps $\Delta\phi$ of the internuclear axis, by applying the corresponding rotation matrix $d^J_{\Omega\Omega}{}^{=3}(\Delta\phi)$ to the $\Omega$-state amplitude vector, typically using $\Delta\phi=\pi/20$. For the $R$ region where $\omega_{\text{prec}} \geq f_L\dot{\phi}$ the $\Omega$-state amplitude vector is kept constant.

The ionization process is interpreted in terms of the exchange mechanism, governed by the overlap of the Ne $(2p)^{-1}$ core hole with the $3p$ core orbital. For the autoionization width $\Gamma(R)$ this results in a two-state basis $\Gamma_\sigma(R)$ and $\Gamma_\pi(R)$ corresponding to the two orientations of the $(2p)^{-1}$ core hole. This approach is a natural extension of the model potential method used successfully to calculate the real part of the optical potential.[16] Both $\Gamma_\sigma$ and $\Gamma_\pi$, depicted in Fig. 4 with a schematic view of the orbital orientations involved, can be described in good approximation by a single exponential function that saturates at small distances. The slope of $\Gamma_\pi$ is larger than for $\Gamma_\sigma$, because the only overlap that contributes to $\Gamma_\pi$ is $\langle(2p)^{-1}\pi_{\text{core}}|(np)\pi\rangle$, where both the angular dependence and the radial dependence contribute to the decrease with increasing $R$ values.

The elements of the $\Omega$-state amplitude vector are decreased by $\exp(-\Gamma^\Omega\Delta t/2\hbar)$ for a time step $\Delta t$ along the trajectory, with

$$\Gamma^\Omega = g_\pi^\Omega\Gamma_\pi(1-g_\pi^\Omega)\Gamma_\sigma \tag{4}$$

and $g_\pi^\Omega$ the relative population of the $\pi$ core states, e.g., $g_\pi=\frac{2}{5}$ for $\Omega=0$ and $g_\pi=1$ for $\Omega=3$.

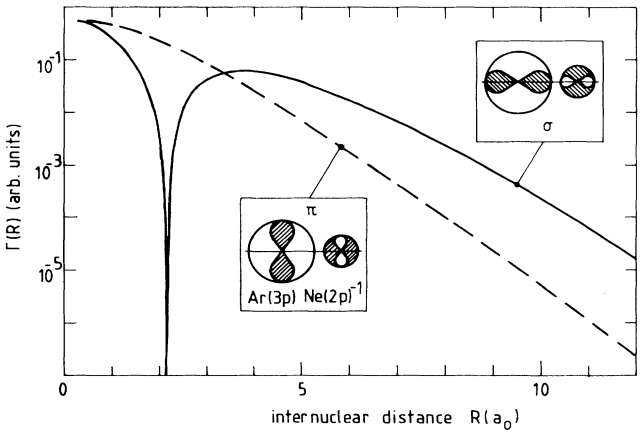


FIG. 4. Calculated results for the basic functions $\Gamma_\sigma$ and $\Gamma_\pi$, using Clementi orbitals of Ar($3p$) and Ne($2p$) as input (Ref. 17). Insets: Two configurations of projectile and target orbitals that contribute.

Finally, we have also included the influence of intramultiplet mixing to the neighboring $\{\alpha\}_8$ and $\{\alpha\}_7$ fine-structure states in the same $\{\alpha\}=\{(2p)^5(3p)\}$ multiplet, with an asymptotic energy difference $\Delta E_{\text{el}}=21$ and 58 meV, respectively.

Numerical results for the polarization effect are given in Table I. For $f_L=0$, i.e., locking at all $R$ values, the polarization effect in the thermal energy range is too large by a factor 2. Moreover, we observe no energy dependence. For $f_L=\infty$, i.e., no locking at all, the polarization effect nearly vanishes over the whole energy range. For $f_L=4\pm1$ we observe a good agreement between the experiment and model calculation.

The agreement of the calculated energy dependence of ${}^3Q_{\text{ion}}$ with the experiment is less accurate. This is due to

TABLE I. Comparison of the experimental results for the polarization effect and the absolute values of the ionization cross section from our semiclassical model calculation, using $f_L=\infty$ (no locking), $f_L=0$ (locking over whole $R$ range), and the best-fit value $f_L=4$ for the locking factor.

| Energy (eV) | ${}^3Q^{0,1}_{\text{ion}}/{}^3Q^3_{\text{ion}}$ Expt.[a] | Expt.[b] | $f_L=\infty$ | $f_L=4$ | $f_L=0$ | ${}^3Q_{\text{ion}}$ (Å$^2$) Expt. | Model |
|---|---|---|---|---|---|---|---|
| 0.075 | 1.69 | 2.12 | 1.27 | 1.77 | 3.40 | 24.5 | 32.3 |
| 0.125 | 1.96 | 2.65 | 1.17 | 1.87 | 4.30 | 23.2 | 28.3 |
| 0.2 | 1.44 | 1.96 | 1.07 | 1.92 | 4.91 | 21.5 | 25.0 |
| 1.0 | 1.24 | 1.59 | 0.88 | 1.31 | 5.30 | 20.2 | 16.1 |
| 2.0 | 1.00 | 1.38 | 0.87 | 0.98 | 4.94 | 26.3 | 12.5 |

[a] ${}^2Q^{0,1}_{\text{ion}}/{}^2Q^2_{\text{ion}}=1$.
[b] ${}^2Q^{0,1}_{\text{ion}}/{}^2Q^2_{\text{ion}}=4/3$.

insufficient information on the repulsive branch of $V^{\Omega}(R)$, which is the basic limitation of this method. Total ionization cross sections are always hampered by a correlation between the absolute scaling of $\Gamma$ and the exact position of the repulsive branch of $V^{\Omega}(R)$.

The result for the locking factor $f_L$ agrees well with the value determined by analyzing polarized-atom cross sections for intramultiplet mixing in the $Ne^{**}(3p)$-He system.[18] Because of the lack of energy-dependent information for the intramultiplet mixing, the evidence is less conclusive. This criterion is confirmed by Grosser[9] in his analysis of the results of $Na^+$ scattering on laser-excited $Na^*(3p)$ atoms of Hertel *et al.*,[1] which also results in $f_L = 4.5 \pm 1$ in our approach.

In this paper we have strong evidence for a semiclassical picture of rotational coupling, including a reliable value for predicting an effective boundary between the limiting cases of a body-fixed or a space-fixed picture of **J**. With respect to the $\Omega$-dependent process of ionization we have proven that a two-state basis for $\Gamma$ is in fair agreement with the polarization effect. In comparison to the analysis of Bussert *et al.*,[5] a considerable reduction of free parameters has been achieved.

This work is supported by the Foundation for Fundamental Research on Matter (FOM).

[1]I. V. Hertel, H. Schmidt, A. Bahring, and E. Meyer, Rep. Prog. Phys. **48**, 375 (1985).

[2]M. O. Hale, I. V. Hertel, and S. R. Leone, Phys. Rev. Lett. **53**, 2296 (1984).

[3]W. Bussert, D. Neuschafer, and S. R. Leone, J. Chem. Phys. **87**, 3833 (1987).

[4]H. A. J. Meijer *et al.*, Phys. Rev. Lett. **59**, 2939 (1987).

[5]W. Bussert *et al.*, J. Phys. (Paris), Colloq. **45**, C1-199 (1985).

[6]M. P. I. Manders, J. P. J. Driessen, H. C. W. Beijerinck, and B. J. Verhaar, Phys. Rev. Lett. **57**, 1577 (1986); Phys. Rev. A **37**, 3237 (1988).

[7]E. E. Nikitin, Adv. Quantum Chem. **5**, 135 (1970).

[8]J. N. L. Connor and K. E. Thylwe, J. Chem. Phys. **86**, 188 (1987).

[9]J. Grosser, Comments At. Mol. Phys. **21**, 107 (1988).

[10]M. H. Alexander and B. Pioully, in *Selectivity in Chemical Reactions,* edited by J. C. Whitehead (Kluwer, Dordrecht, 1988), p. 265.

[11]M. F. Verheijen and H. C. W. Beijerinck, Chem. Phys. **102**, 255 (1986).

[12]F. T. M. van den Berg, J. H. M. Schonenberg, and H. C. W. Beijerinck, Chem. Phys. **115**, 359 (1987).

[13]J. P. J. Driessen, M. F. M. Janssens, and H. C. W. Beijerinck, contribution to Seventh European Conference on Dynamics of Molecular Collisions, Assisi (Perugia) Italy, 5–9 September 1988 (unpublished).

[14]T. Bregel, in *Electronic and Atomic Collisions,* edited by D. C. Lorents, W. E. Meyerhof, and J. R. Peterson (North-Holland, Amsterdam, 1986), p. 577.

[15]R. W. Gregor and P. E. Siska, J. Chem. Phys. **74**, 1078 (1981).

[16]D. Hennecart and F. Masnou-Seeuws, J. Phys. B **18**, 657 (1985).

[17]E. Clementi, "Tables of Atomic Functions," supplement to IBM J. Res. Dev. **9**, 2 (1965).

[18]M. P. I. Manders, W. B. M. van Hoek, E. J. D. Vredenbregt, G. J. Sandker, H. C. W. Beijerinck, and B. J. Verhaar, Phys. Rev. A **39**, 4467 (1989).